Pilot Sensitivity to Simulator Flight Dynamics Model Formulation for Stall Training

Kevin Cunningham,[1] Gautam H. Shah[2], Patrick C. Murphy[3]
NASA Langley Research Center, Hampton, VA, 23681

Melissa A. Hill,[4] and Brent P. Pickering[5]
Unisys Corporation, NASA Langley Research Center, Hampton, VA, 23681

A piloted simulation study was performed in the Cockpit Motion Facility at the National Aeronautics and Space Administration Langley Research Center. The research was motivated by the desire to reduce the commercial transport airplane fatal accident rate due to in-flight loss of control. The purpose of this study, which focused on a generic T-tail transport airplane, was to assess pilot sensitivity to flight dynamics model formulation used during a simulator stall recognition and recovery training/demonstration profile. To accomplish this, the flight dynamics model was designed with many configuration options. The model options were based on recently acquired static and dynamic stability and control data from sources that included wind tunnel, water tunnel, and computational fluid dynamics. The results, which are specific to a transport airplane stall recognition and recovery guided demonstration scenario, showed the two most important aerodynamic effects (other than stick pusher) to model were stall roll-off and the longitudinal static stability characteristic associated with the pitch break.

I. Nomenclature

Aero.	=	aerodynamic	deg or °	=	degrees
AoA	=	angle of attack	Dyn.	=	dynamic
a, b_1	=	deficiency function parameters	Dyn. Stab.	=	dynamic stability
b	=	wingspan, feet	FAA	=	Federal Aviation Administration
CAS	=	calibrated airspeed, knots	GTT	=	Generic T-tail Transport
CAST	=	Commercial Aviation Safety Team	g	=	acceleration due to gravity
CFD	=	computational fluid dynamics	Ixx	=	moment of inertia about longitudinal axis, slug-ft^2
C_l	=	rolling moment coefficient	Iyy	=	moment of inertia about lateral axis, slug-ft^2
C_m	=	pitching moment coefficient	Izz	=	moment of inertia about normal axis, slug-ft^2
C_{m_q}	=	pitch damping coefficient, per radian	NASA	=	National Aeronautics and Space Administration
Ctrl.	=	control	NTSB	=	National Transportation Safety Board
$\bar{c}$	=	mean aerodynamic chord, feet			

[1] Senior Research Engineer, Flight Dynamics Branch, Mail Stop 308, AIAA Senior Member.
[2] Senior Research Engineer, Flight Dynamics Branch, and Manager, TASA, MS 308, AIAA Associate Fellow.
[3] Senior Research Engineer, Dynamic Systems & Controls Branch, MS 308, AIAA Associate Fellow.
[4] Software Engineer, NASA Langley Research Center, Mail Stop 169.
[5] Software Engineer, NASA Langley Research Center, Mail Stop 169.

q	=	body axis angular rate, pitch axis	α	=	angle of attack, degrees
$\hat{q}$	=	$q\bar{c}/2V$	$\dot{\alpha}$	=	angle of attack rate of change, degrees/sec
rad	=	radian	β	=	sideslip angle, degrees
RWD	=	right wing down	Δ	=	incremental change
S	=	wing area, feet^2	δ_c	=	percent control column deflection
SE	=	Safety Enhancement	δ_{wheel}	=	percent control wheel deflection
sec	=	seconds	θ	=	pitch attitude angle, degrees
TASA	=	Technologies for Airplane State Awareness	ϕ	=	bank angle, degrees
V	=	velocity			

II. Introduction

In-flight loss of control has historically been a major contributor to the fatal accident rate of commercial transport airplanes [1]. A key intervention strategy that aims to reduce the occurrence of loss-of-control accidents is the improvement of flight simulations to allow for a more accurate representation of stalls, loss-of-control, and upset scenarios [2]. The potential uses for the improved simulations include control law analysis, advanced flight display design, mishap investigation, engineering support, and training for recognition and recovery from full stall conditions. The National Aeronautics and Space Administration (NASA) published research on this topic in 2002 [3]. At that time, a NASA/Boeing partnership, operating under NASA's Aviation Safety Program, performed extensive aircraft accident analysis, simulation technology analysis, ground-based aerodynamic testing, and flight simulation development to address the potential for improving transport airplane simulations for use in stall and upset conditions [4]. The focus vehicle for that configuration was a single-aisle transport airplane with a conventional horizontal tail (mounted low relative to the vertical tail, as opposed to a T-tail configuration).

In 2009, the National Transportation Safety Board (NTSB) investigated a fatal mishap involving in-flight loss of control of a twin engine turbo-prop commercial transport airplane. The NTSB determined the probable cause of that mishap to be an inappropriate response to a stall warning system, which resulted in an aerodynamic stall from which the airplane did not recover. In their investigative report [5], the NTSB cited research by NASA/Boeing and others relating to modeling and simulation of stalled flight conditions. One of the report's recommendations (A-10-24) called for defining simulator fidelity requirements and addressing other requirements to support full stall recovery training during flight simulator training.

After publication of NTSB recommendation A-10-24, a public law (111-216) was passed in 2010, which requires stall training for all Part 121 air carriers. To meet the requirements of that law, the Federal Aviation Administration (FAA) developed rules and regulations that will result in full stall simulator training beginning in 2019 [6]. During this developmental phase, the FAA [7], and others investigated model fidelity requirements relating to the use of simulation of transport airplane stall characteristics. That investigation focused on several stall models representing an airplane with wing-mounted engines and a low horizontal tail.

Expanding research efforts to include the study of stall model fidelity pertaining to T-tail airplanes with aft twin engines was identified as a safety enhancement element by the Commercial Aviation Safety Team (CAST). CAST is a government-industry partnership with a strategy to reduce commercial aviation fatality risk. CAST working groups use accident analysis to identify plans for potential changes to prevent accidents. These formally adopted plans take the form of Safety Enhancements (SE). SE-209 is the specific CAST research-based Safety Enhancement that includes an element to investigate flight dynamics models of a T-tail airplane with aft twin engines.

To contribute toward the model fidelity research goals of SE-209, NASA has conducted dedicated high-angle-of-attack ground testing of a generic T-tail transport (GTT) airplane configuration [8]. Multiple experimental facilities and computational fluid dynamics (CFD) codes were utilized for this research. The test techniques that were used included static and dynamic force and moment testing as well as flow visualization. Data from these tests were used to develop a six-degree-of-freedom simulation model.

This paper extends the body of knowledge (from Ref. [7]) by examining detailed aspects of a high fidelity flight dynamics model. In particular, it addresses which model attributes a pilot is most sensitive to when flying a profile that could be used to demonstrate a range of stall characteristics in an extended envelope aerodynamic database.

III. Descriptions

A. The Generic T-tail Transport (GTT) Simulator

A brief description of the GTT will be provided here. Details of the simulator and flight dynamics model may be found in Ref. [8] and Ref. [9] respectively.

The GTT simulation was implemented by the Simulation Development and Analysis Branch at NASA Langley Research Center in Hampton, Virginia. The GTT simulation model represents a T-tail transport airplane with a 76-foot wingspan and 98-foot fuselage length. The nominal center of gravity (and moment reference location) is the 25% mean aerodynamic chord location. The nominal mass properties of the configuration are intended to represent the airplane at a light weight (6,000 pounds of fuel). Aerodynamic reference dimensions and the GTT baseline mass properties are shown in Tables 1 and 2. The propulsion system integrates models of two 14,000-pound-thrust-class turbofan engines developed at the NASA Glenn Research Center in Cleveland, Ohio. A sketch of the GTT geometric configuration and control surface arrangement is shown in Fig. 1. Drawings with higher detail are shown in Ref. [8].

Table 1. Aerodynamic reference dimensions.

Aerodynamic Reference	Symbol	Full Scale Dimension
Mean Aerodynamic Chord	$\bar{c}$	11.07 feet
Wingspan	b	75.98 feet
Wing Area	S	754.32 feet^2

Table 2. Mass properties.

Parameter	Quantity	Units
Weight	55,847	pounds
Ixx	175,849	slug-foot^2
Iyy	1,114,179	slug-foot^2
Izz	1,266,792	slug-foot^2

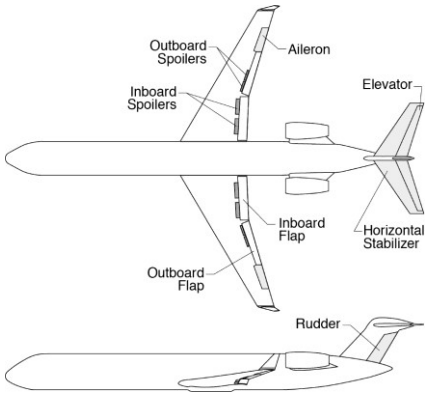

Fig. 1 A sketch of the GTT configuration showing control surface arrangement.

The simulator used for this study is shown in Figs. 2 and 3. Figure 2 is an exterior view of the simulator cockpit and 76-inch, six-degree-of-freedom, hydraulically-actuated synergistic hexapod motion system. Figure 3 is a photograph showing the interior of the flight deck simulator. It is configured as a modern transport airplane with a full suite of flight deck panels, a center aisle stand and throttle quadrant, and flight management computer.

The cockpit control inceptors consist of two sets of wheel-columns and pedals that are fully back-driven in all axes via an electric control loading system. This provides dynamic feedback to the pilot(s) with force-feel profiles tuned for the GTT vehicle. In addition to simulating flight control feedback, the control loader is used to simulate the stick pusher mechanism. Each column is also equipped with a hardware stick shaker that is triggered by the simulated stall warning system.

Fig. 2 A photograph showing the exterior of the simulator cockpit mounted on a hexapod motion base.

Fig. 3 A photograph showing the interior of the GTT simulator cockpit.

B. Flight Dynamics Model Options

For this investigation, the GTT simulation flight-dynamics model was implemented with a baseline configuration and numerous options for varying the model. The baseline model was designed to be a high fidelity flight-dynamics model which could be used during guided training and demonstration of full stall characteristics of this GTT airplane simulation. The purpose of the model options was to allow the pilot to compare the effects of the options to the baseline. This was accomplished by having a pilot first fly a profile with the baseline configuration, then fly a second profile using an optional configuration. The model options that were studied are summarized in Table 3 and described in the numbered sections immediately following.

Table 3. Configurable options for the GTT simulation flight dynamics model.

Model Options	Baseline	Modification
Stick Pusher	Disabled	Enabled
Aerodynamic Asymmetries	Enabled	Disabled
Control Effectiveness	Modeled to high AoA (60°)	Modeled only to stall warning AoA (7.5°)
Longitudinal Static Stability (at stall)	Gradual pitch up	Abrupt pitch up
Dynamic Stability	Linear with rate and nonlinear with AoA	Linear with rate and constant with AoA
		Nonlinear with rate and nonlinear with AoA
Unsteady Aerodynamic Effects	Disabled	Enabled

1. *Stick Pusher*

Because the focus of this study was on the natural aerodynamic characteristics of the focus vehicle, the baseline configuration for the stick pusher option was "disabled". When the stick pusher was enabled, activation would occur when angle of attack exceeded a threshold (10 degrees). Upon activation, a 65-pound column-forward force would be applied. This produced an approximate 10 degree trailing-edge-down elevator deflection and typically resulted in a recovery profile in which the normal load factor never decreased below 0.5 g. The stick pusher deactivated when (low-pass filtered) angle of attack decreased below the threshold value.

2. *Stall Asymmetries*

The baseline configuration for the asymmetry model was "enabled." This means that by default, a representation of aerodynamic asymmetries attributed to high-angle-of-attack conditions was active. Increments to rolling moment, yawing moment, and side force coefficients were superimposed using two-dimensional table lookup functions, which were dependent on angle of attack and angle of sideslip. The initial stall asymmetry onset angle of attack was 9 degrees. To assess the importance of this effect, the stall asymmetry option could be disabled so that a comparison with the baseline configuration could be performed. The rolling moment coefficient increment attributed to aerodynamic stall asymmetry is shown by a red line in Fig. 4.

3. *Control Effectiveness*

The baseline configuration for the flight control effectiveness was modeled as a function of angle of attack across the entire angle of attack range (-8 to 60 degrees) of the database. When set to the modified option, the degradation in control effectiveness above the stall warning angle of attack (7.5 degrees) was not represented, and simply held constant. This approach, which was applied to all surfaces and incremental effects, is illustrated in Fig. 4 for the incremental effect of full aileron deflection on rolling moment coefficient.

4. *Longitudinal Static Stability*

Baseline and modified pitching moment characteristics are shown in Fig. 5. These two characteristics were used for pilot evaluation of the change in the longitudinal static stability, most notably in the range of 16 to 18 degrees angle of attack. The baseline characteristic was based on measurements (tunnel and computational) acquired for a low Reynolds Number (about 250,000 based on chord) condition. The modified characteristic was obtained from computational fluid dynamics solutions at flight Reynolds Number (about 16,000,000 based on chord). The low Reynolds Number data were used as the baseline in this study because a comprehensive set of static, dynamic, and control effects data were available at a consistent Reynolds Number. High Reynolds Number characteristics were only estimated using computational fluid dynamics for a very limited data set. For this study it was important to have a baseline with the various stability and control characteristics degrading in a synchronous manner as angle of attack increased. Hence the low Reynolds Number data set was used as the baseline, and the effect of this limitation was assessed by the comparison.

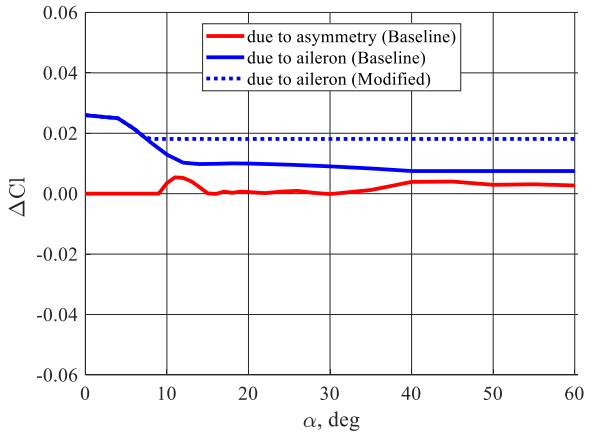

Fig. 4 Examples of incremental rolling moment coefficients models for the stall asymmetry and aileron control effectiveness options.

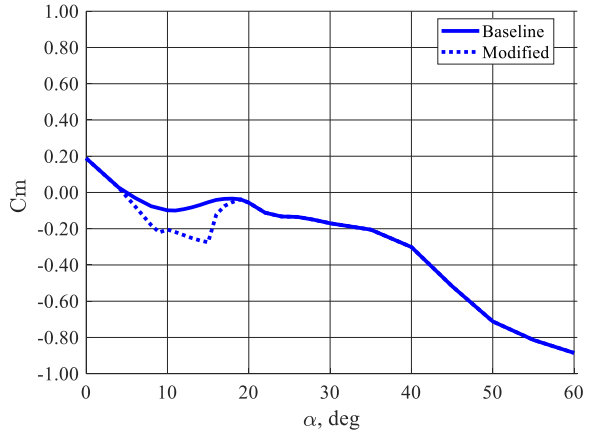

Fig. 5 Baseline and modified pitching moment characteristics.

5. *Dynamic Stability*

This study used three options to represent dynamic stability. The baseline configuration represented dynamic stability coefficients as linear derivatives (with respect to rate) which varied as a tabulated function of angle of attack (Fig. 6). This is a common form used in flight simulators. The stability derivative characteristics were derived from tunnel tests and augmented with computational fluid dynamic results (Ref. [8]).

Two options were used for comparison against the baseline. One was simpler, the other was more complex. The simpler option used a single constant value for each of the various dynamic stability derivatives over the entire angle-of-attack range (Fig. 6). That single derivative value was obtained from a normal slow flight condition (5 degrees angle of attack) and represents an approach that may have been used in some heritage transport airplane training simulations (Ref. [4]). Figure 7 shows an example of the more complex option representing the dynamic stability coefficients as two-dimensional functions which were dependent on angle of attack and body axis rate (detailed in Ref. [9]).

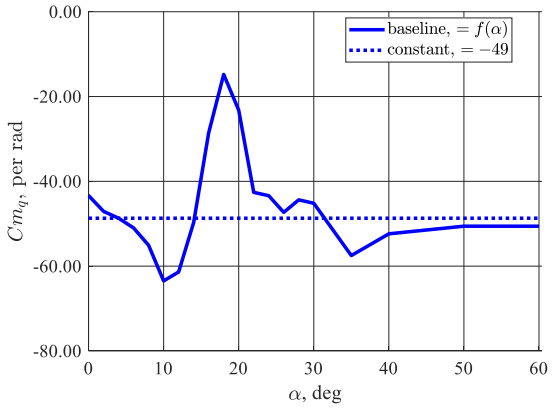

Fig. 6 Pitch damping coefficient is shown as an example of two of the optional forms for the dynamic stability model (one a linear derivative which varies with angle of attack and the other, a linear derivative which remains constant for all angles of attack).

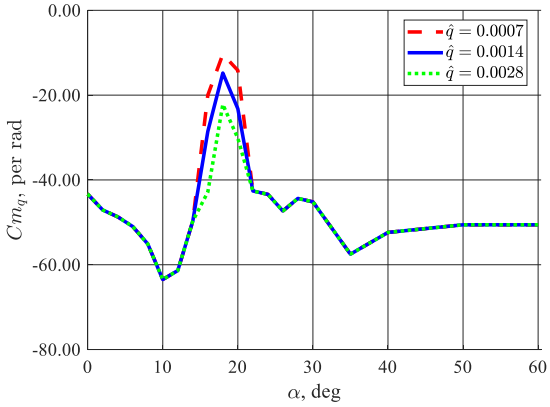

Fig. 7 Pitch damping coefficient is shown as an example of the third optional form for the dynamic stability model (a function of both angle of attack and rate).

6. *Unsteady Aerodynamic Effects*

The baseline configuration for the unsteady aerodynamic model was "disabled". When enabled, the unsteady model adds higher fidelity responses to the simulation. Several new terms are computed for addition into the classic force and moment coefficient buildup equations. These aerodynamic terms are included with the conventional series expansions of the aerodynamic forces and moments. However, stability coefficients related to $\dot{\alpha}$ are replaced by their unsteady equivalent, $a\eta(t)$, where unsteady behavior is present. For example, the pitching moment basic linear state space representation can be written as

$$\dot{\eta}(t) = -b_1\eta(t) + \dot{\alpha}(t)$$
$$C_m(t) = C_{m0} + C_{m_\alpha}(\infty)\alpha(t) + \frac{\bar{c}}{2V}C_{m_q}(\infty)q(t) - a\eta(t) \quad (1)$$

The two new parameters, a and b_1, define a transfer function that comes into play (for each degree of freedom) and can be thought of as a gain and a lag in the unsteady response.

For this experiment with the GTT simulation model, only the pitching moment equation was modified. The parameters for the modification were based on specialized sinusoidal forced oscillation testing conducted in a water tunnel to characterize the unsteady and nonlinear damping. When the unsteady aerodynamic effects model was enabled, the net effect was a destabilization of the dynamic stability and an increased lag in the pitch damping. Complete details of the modeling approach can be found in Refs. [10, 11].

IV. Approach

A. Pilot Evaluation Experimental Procedure

The purpose of the study was to assess which flight dynamics model options were, by pilot opinion, most important for use in a full stall demonstration profile. This was accomplished by asking a group of pilots to perform full stalls in the simulator first using the reference (baseline) flight dynamics model, then repeating the task using a model variant which was being evaluated. They were informed that their stall recovery performance was not being evaluated and to focus their attention on the stability and control characteristics during the stall. The pilots were instructed (and received training) to provide their evaluation after the second of the two runs being compared. The evaluation instructions were also placarded in two locations in the cockpit for their reference:

1. What, if anything, was different? (evaluation stall compared to the reference stall)
2. Rate the difference (0 to 9, integer only):
    - 0: nothing was different
    - 1 – 3: small differences / low importance for stall training
    - 4 – 6: medium differences / medium importance for stall training
    - 7 – 9: large differences / high importance for stall training

Eight pilots were included in this study. The primary requirement for inclusion into the study was that each individual be a licensed pilot (at a minimum holding a private pilot license) and have had formal training in airplane stability and control. All of the pilots had experience as either flight test professionals (pilots or engineers) or research engineers. Pilots with technical backgrounds and stability and control education were sought because the focus of this research was on stability, control, and handling characteristics (as opposed to aircraft operating procedures).

The pre-simulator session pilot briefing included background information, a review of flight displays, flight profiles and procedures, evaluation comment and rating instructions, schedule, and safety information. Upon arrival in the cockpit, the pilot was shown the location of the comment/rating placards. The pilot was the sole occupant of the cockpit during the simulator session. The pilot communicated with simulation operators and a researcher (as needed), using a “hot microphone” intercom communications link. Pilot ratings and comments were recorded.

B. Evaluation Profile

All simulator runs, both baseline reference and evaluation, used the same profile. The flight profile began with the GTT simulation trimmed in level flight at 10,000 feet above mean sea level and 180 knots calibrated airspeed. The profiles were all flown in standard day atmospheric conditions with very light turbulence. The simulator was configured for the nominal mass properties shown in Table 2 with the center of gravity set for 25 percent mean aerodynamic chord. The pilots were instructed to refrain from using stabilizer trim, throttle, or rudder. The purpose of these instructions was to improve repeatability and consistency of results.

The pilots were instructed to maintain wings level while tracking a pitch attitude reference bar (shown at 5 degrees attitude in Fig. 8). Three seconds into the run, the bar would steadily ramp from 5 to 10 degrees pitch attitude over a period of 13 seconds. It would maintain the reference target pitch attitude at 10 degrees until recovery was initiated, at which time the reference bar would be removed from the display. The pilots were instructed that a message on the primary flight display would appear to notify them when to recover (Fig. 9). They were briefed that this would always trigger automatically when angle of attack exceeded a post-stall threshold (full stall + 12 degrees). The recovery threshold value was set to ensure coverage of the angle-of-attack range of a hypothetical minimally extended envelope training package (for this generic vehicle). For experimental consistency, the pilots were briefed to use a controls-neutral (hands-off) recovery strategy.

Two profiles were always flown back-to-back: first with the flight dynamics model configured with reference (baseline) settings and second with the model reconfigured with options under evaluation. The pilots were not informed what features were being evaluated. However, they were advised immediately prior to the single run which enabled the stick pusher and were reminded not to oppose or "fight" operation of the device. The runs were generated in a (one time) random order, but all pilots were given the same randomized sequence due to the small sample size. Each experimental option specified in Table 3 was flown only one time (to minimize fatigue). Five baseline runs (repeats) were inserted into the matrix in addition to the experimental conditions to determine the threshold of the pilot's ability to recognize identical scenarios.

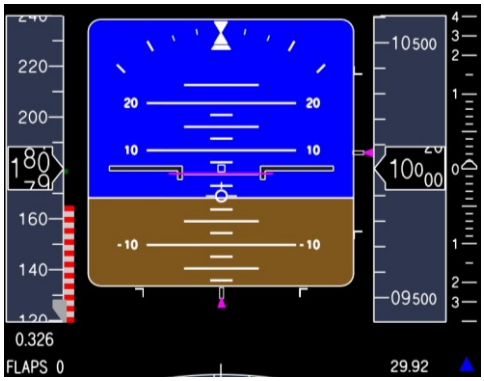

Fig. 8 An illustration of the primary flight display in normal flight mode. Note the magenta bar providing a pitch attitude reference target located at 5 degrees pitch attitude.

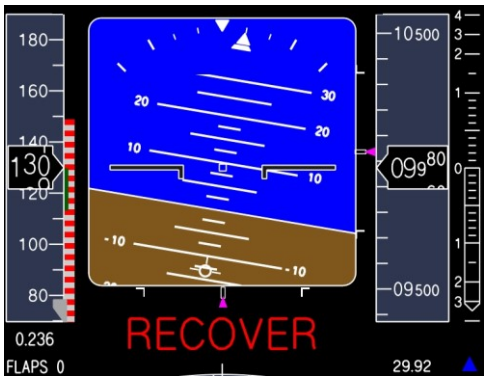

Fig. 9 An illustration of the display with the visual annunciation used to inform the evaluation pilot to apply recovery inputs.

V. Results

The results of the pilots' subjective assessment of seven flight dynamics model variations are presented in this report. The data from each individual pilot were acquired during a single 2.5-hour simulator session (nominally 1.1 hours in the cockpit). Pilots initially performed a block of runs for familiarization with the profile and displays. The familiarization profile runs were flown using the baseline flight dynamics model configuration. The pilots were allowed to take as many runs as they desired. They were asked to repeat the profile until they felt comfortable with the profile, displays, procedures and normal run-to-run variations. The pilots generally used six runs for familiarization.

To limit pilot fatigue, the baseline configuration was the only configuration for which each pilot performed repeat evaluations. This was important because the back-to-back repeats could appear to be quite different for several reasons. The primary reason was due to the instability of some static aerodynamic characteristics above the full stall angle of attack. Thus, minor deviations in control inputs or pilot reaction could result in significantly different trajectories. The secondary reason was apparent randomness included in the stall asymmetry model. For this study, the randomness was limited to changes to the sign of the increments representing the stall asymmetries. The random sign change was applied uniformly to all the asymmetry increments at the start of the runs. No random changes were applied to the magnitude of the asymmetry characteristics. A pilot with perfect ability to characterize the stall profile characteristics and to perfectly account for any asymmetry randomness would have always rated the baseline repeats "0", meaning no difference between the evaluation run and the baseline configuration that immediately preceded it. The median rating (all eight pilots, each with five baseline repeats) was 2. This suggests that any model variation which was rated less than or equal to 2 may be no more apparent (to the pilot) than baseline repeatability.

Figures 10 – 12 are plots showing typical time history responses for the evaluation profiles which were run in the simulator using the baseline flight dynamics model options. Figure 10 shows longitudinal parameters of interest. These data show the pilot ramping up the pitch attitude then maintaining a 10 degree pitch attitude as angle of attack is allowed to increase (throttle and stabilizer were invariant during all runs). For reference, the stall warning (stick shaker) angle of attack was set at 7.5 degrees and the stall protection (stick pusher) activation angle of attack was 10.0 degrees. (Recall that the stick pusher was disabled in the baseline configuration.) The recovery annunciation was triggered when angle of attack exceeded 22.0 degrees. Figure 11 shows bank angle, sideslip angle, and wheel input. Between stick shaker (7.5 degrees) and full stall angle of attack (10 degrees) small wheel inputs were required to control bank angle. As angle of attack increased past full stall, sideslip angle further increased due to decreasing yaw damper effectiveness, decreasing control effectiveness, and decreasing lateral-directional static stability. Significantly more wheel input was applied as the pilot attempted to control the bank angle after full stall. When recovery inputs were applied at approximately 62 seconds, angle of attack quickly decreased and the airplane rolled left wing down due to sideslip angle coupled with strong, stable dihedral effect (Ref. 9). Figure 12 shows the airspeed and altitude exchange during the profile. Nominally, a 3,000-foot altitude loss was observed from the time recovery was initiated until a positive climb condition was attained (throttle position was invariant during the entire profile).

Figure 13 graphs the median pilot ratings of the impact of the various flight dynamics model effects (Table 3) that were tested. The subjective ratings reflect the pilot's opinion of the difference between the model under evaluation and the baseline model. Pilots were instructed to consider their rating of the stability and control differences in the context of application to a simulation-based stall recognition and recovery training mission.

Although the stick pusher has an artificial effect on the stall characteristics, Fig. 13 shows the pilots viewed it as the most important difference. One pilot comment summarized the effect as "…it completely changes the character of the stall." Other pilot comments also noted that the implementation details of the pusher (hysteresis) is considered important because if the pusher allows more airspeed to build before disengaging, there would be lower tendency to pull to a secondary stick shaker activation. One pilot (correctly) noted that there was a slight roll off beginning immediately prior to pusher activation.

Stall asymmetry was also rated relatively high. Pilot comments frequently characterized it as "significant". Other pertinent comments noted changes in apparent stability, workload, and the amount of uncommanded motion. While discussing the absence of a stall asymmetry model, one pilot commented: "…significant because it was one dimensional … as far as handling qualities, I'd say it isn't what you want."

For the assessment of changes to the longitudinal static stability characteristics, Fig. 5 shows the modified static stability characteristics that were compared to the baseline characteristics. Figure 13 shows that the evaluation pilots clearly noted the difference and considered it a medium difference. All pilots either commented on pitch controllability or commented on the larger pitch up (pitch up was the most frequent comment). While explaining a medium level rating, one pilot elaborated that the change wasn't presenting a new characteristic and didn't change his ability to recognize the stall pitch up, it just made the existing characteristic more obvious.

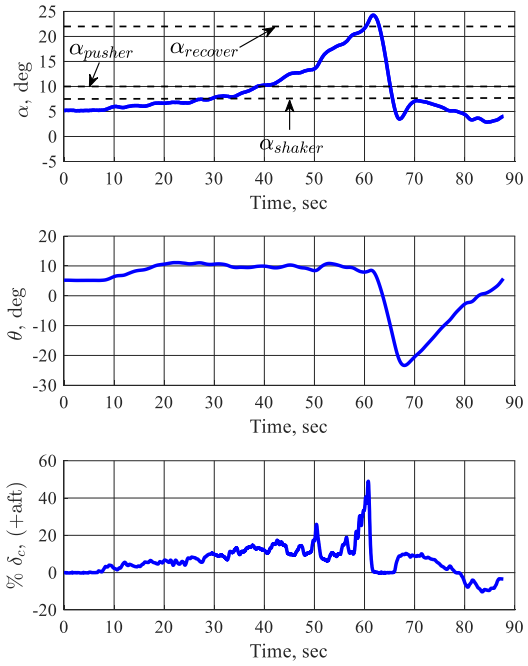

Fig. 10 Time history plots of control column inputs and responses for a typical evaluation profile using the baseline flight dynamics model.

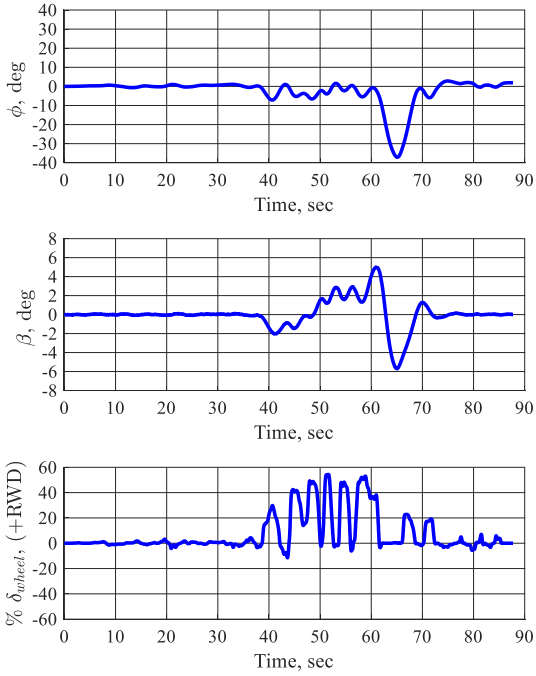

Fig. 11 Time history plots of control wheel inputs and responses for a typical evaluation profile using the baseline flight dynamics model.

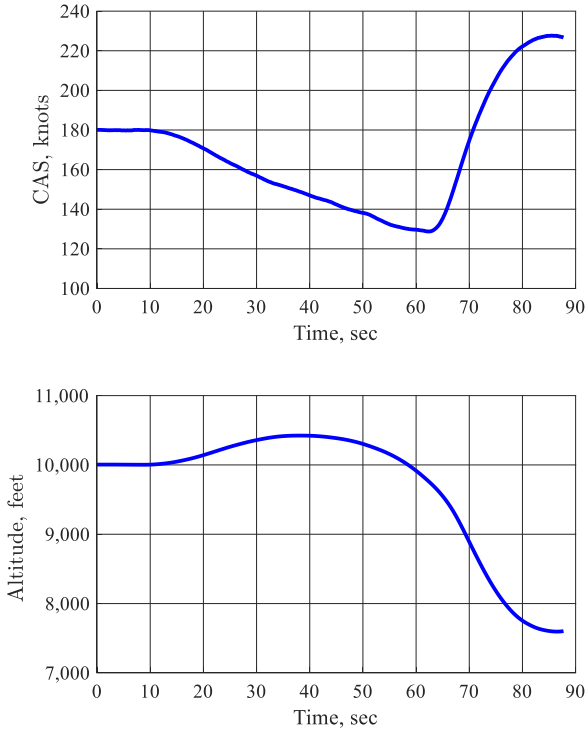

Fig. 12 Time history plots of calibrated airspeed and altitude during a typical evaluation profile using the baseline flight dynamics model.

To investigate dynamic stability model formulation, the baseline model, in which linear derivatives varied with angle of attack, was replaced with a form in which linear derivatives were invariant with angle of attack. (See Fig. 13, "Dynamic Stab = f(AoA)"). The invariant linear derivative option represented dynamic stability characteristics from the normal flight envelope and omitted the extended envelope effects. While assessing this, the pilots generally recognized that something had changed and considered that it was a moderate difference. About half commented on the change in the oscillatory nature of the response and the other half focused their comments on the amount of wheel input which was required to counter the stall asymmetry. These comments occurred because of the artificially higher damping that was encountered at post-stall angle of attack.

The modification to control effectiveness artificially increased the effectiveness in the stall regime. Pilot comments relating to this scenario were mixed. Half the pilots failed to attribute the difference to controls or controllability. Of the remaining four, all noted that the vehicle was easier to control, and two expressed uncertainty about a change in control effectiveness. Only one of the pilots definitively stated that control effect had changed (because a change in maximum wheel position was apparent). Most of the pilots considered the effect to be of medium or small importance. The median rating was 3, falling inside the "small change" category of Fig. 13.

The assessment of unsteady aerodynamic model effects and the assessment of dynamic stability modeled as a function of both angle of attack and rate yielded median ratings of 2 and 1 respectively. Those ratings were at and below the median rating for the baseline repeats. Thus, they are considered to be unimportant for the flight dynamics model of this generic vehicle when this task is performed. Pilot comments for these model options were consistent with the median ratings shown in Fig. 13, which is to say the comments were generally vague and most frequently stated that little if any difference was perceived.

The finding that the unsteady aerodynamic model effects and the dynamic stability model in a form which includes both rate and angle effect variation is perhaps the most important result for this configuration. It is important because both of these approaches are more complex (and thus costly) than the traditional methods used to represent transport airplane dynamic characteristics at high angle of attack. The results suggest that applying the traditional methods over an extended angle of attack range was generally an effective approach to attain pilot recognition of the enhanced dynamic response.

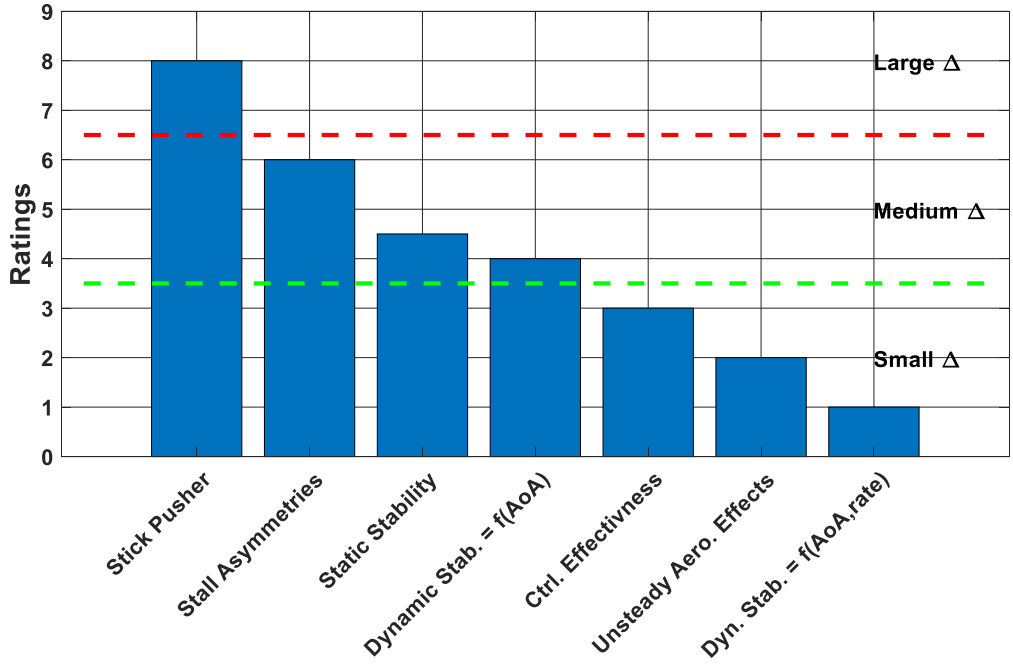

Fig. 13 Subjective pilot ratings of perceived stall stability and control characteristics differences for flight dynamics model variations.

VI. Concluding Remarks

This study used the NASA GTT simulation model to obtain pilot opinion on the relative importance of a set of flight dynamics model options for recognition of stall-related stability and control characteristics during stall and post-stall flight simulation. The test was performed in the NASA Langley Cockpit Motion Facility. A hexapod motion base with stall-buffet modeling was used. This study was limited to a maximum angle of attack of approximately 12 degrees above full stall. Only 25 percent mean aerodynamic chord center of gravity location and flaps up configuration were considered. Also, the pilot application of thrust changes, trim changes, and rudder inputs were not considered.

The consensus opinion of the eight evaluation pilots indicated that implementation of a stick pusher system's mechanization was the most important change to implement (relative to a baseline flight dynamics model). This is attributed to the dramatic way in which the system redefined the generic T-tail airplane's stall characteristic (an unstable pitch up to an apparent crisp, stable, nose down pitch break). In the absence of an active stick pusher system, the consensus was that the next most important effect to model was aerodynamic asymmetries (e.g. roll off) associated with stall. Pilot comments indicated that when this effect was not modeled, straight ahead stalls were very different because lateral-directional dynamics did not become excited and thus did not further challenge pilot workload.

The consensus also indicated that more advanced models associated with unsteady aerodynamics effects and the effect of rate on dynamic stability were not of significant importance (for this configuration and task). This is important because these models are more complex than the standard approaches used in transport airplane simulations and the increased complexity could lead to greater development and implementation costs. Pilot opinion in this study suggested that traditional simulation modeling methods were adequate for the tasks.

Of medium to low importance were the treatments of static stability, dynamic stability (using traditional linear derivatives, scheduled with angle of attack), and flight control effectiveness.

Results of this study can only be considered relevant for a transport airplane configuration conducting a full stall demonstration profile or full stall recognition and recovery training.

Acknowledgments

This work was funded under the Safety Enhancement 209 Element of the Technologies for Airplane State Awareness Sub-project of the System-Wide Safety Project. That project is part of the NASA Aeronautics Research Mission Directorate's Airspace Operations and Safety Program.

VII. References

[1] "Statistical Summary of Commercial Jet Airplane Accidents: Worldwide Operations 1959-2015.", Boeing Commercial Airplanes. Seattle, Washington, July 2016.

[2] Crider, Dennis A., "The Use of Data from Aviation Accident Investigations in Development of Flight Simulator Training Scenarios", AIAA 2017-1078, AIAA Modeling and Simulation Technologies Conference, AIAA SciTech Forum, January, 2017.

[3] Shah, Gautam H., et al., "Wind-Tunnel Investigation of Commercial Transport Aircraft Aerodynamics at Extreme Flight Conditions", SAE 2002-01-2912, World Aviation Congress & Display, November 5-7, 2002.

[4] Foster, John V., et al., "Dynamics Modeling and Simulation of Large Transport Airplanes in Upset Conditions", AIAA 2005-5933, August, 2005.

[5] "Loss of Control on Approach, Colgan Air, Inc., Operating as Continental Connection Flight 3407, Bombardier DHC-8-400, N200WQ, Clarence Center, New York, February 12, 2009," Accident Report NTSB/AAR-10/01, National Transportation Safety Board, Washington DC, Feb. 2010.

[6] Schroeder, Jeffery A. and Burke, Robert H., "Upset Prevention and Recovery Training – A Regulator Update", AIAA 2016-1429, 4 January, 2016.

[7] Schroeder, Jeffery A., et al., "An Evaluation of Several Stall Models for Commercial Transport Training", AIAA 2014-1002, AIAA Modeling and Simulation Technologies Conference, AIAA SciTech Forum, January, 2014.

[8] Cunningham, K., Shah, G. H., Frink, N. T., McMillin, S. N., Murphy, P. C., Brown, F. R., Hayes, P. J., Shweyk, K. M., Nayani, S. N., "Preliminary Test Results for Stability and Control Characteristics of a Generic T-tail Transport Airplane at High Angle of Attack", AIAA 2018-0529, AIAA Atmospheric Flight Mechanics Conference , AIAA SciTech Forum, January, 2018.

[9] Cunningham, K., Shah, G. H., Hill, M. A., Pickering, B. P., Litt, J. S., Norin, S. B., "A Generic T-tail Transport Airplane Simulation for High-Angle-of-Attack Dynamics Modeling Investigations", AIAA 2018-1168, AIAA Modeling and Simulation Technologies Conference, AIAA SciTech Forum, January, 2018.

[10] Murphy, P. C., Frink, N. T., McMillin, S. N., Cunningham, K., Shah, G. H., "Efficient Unsteady Model Estimation Using Computational and Experimental Data", AIAA 2018-3622, AIAA Atmospheric Flight Mechanics Conference, AIAA Aviation Forum, June, 2018. DOI: 10.2514/6.2018-3622

[11] Murphy, P. C., Frink, N. T., McMillin, S. N., Cunningham, K., Shah, G. H., "Unsteady Model Estimation for Generic T-Tail Transport Aircraft Using Computational Data", (To be published), AIAA Atmospheric Flight Mechanics Conference, AIAA SciTech Forum, January, 2019.